Analytic models for density of a ground–state spinor condensate

2 authors:

Sandeep Gautam
Indian Institute of Technology Ropar
32 PUBLICATIONS   **232** CITATIONS

SEE PROFILE

Sadhan K. Adhikari
São Paulo State University
276 PUBLICATIONS   **4,539** CITATIONS

SEE PROFILE

Analytic models for density of a ground-state spinor condensate

Sandeep Gautam[*1] and S. K. Adhikari[†1]

[1]Instituto de Física Teórica, Universidade Estadual Paulista - UNESP,
01.140-070 São Paulo, São Paulo, Brazil

We demonstrate that the ground state of a trapped spin-1 and spin-2 spinor ferromagnetic Bose-Einstein condensate (BEC) can be well approximated by a single decoupled Gross-Pitaevskii (GP) equation. Useful analytic models for the ground-state densities of ferromagnetic BECs are obtained from the Thomas-Fermi approximation (TFA) to this decoupled equation. Similarly, for the ground states of spin-1 anti-ferromagnetic and spin-2 anti-ferromagnetic and cyclic BECs, some of the spin component densities are zero which reduces the coupled GP equation to a simple reduced form. Analytic models for ground state densities are also obtained for anti-ferromagnetic and cyclic BECs from the TFA to the respective reduced GP equations. The analytic densities are illustrated and compared with the full numerical solution of the GP equation with realistic experimental parameters.

PACS numbers: 03.75.Mn, 03.75.Hh, 67.85.Bc, 67.85.Fg

I.   INTRODUCTION

The advent of the optical traps paved the way for the first realization of a Bose-Einstein condensate (BEC) with internal spin degrees of freedom [1], also known as a spinor BEC. Since then, a lot of theoretical and experimental studies have been performed on the spinor BECs [2–4]. In contrast to a scalar BEC, which is characterized by a single interaction parameter, the spin-1 [5] and spin-2 [6, 7] BECs have, respectively, two and three interaction parameters. Depending on the relative strength of the interaction parameters, a spin-1 BEC in the absence of external magnetic field can be either in a *ferromagnetic* or an *anti-ferromagnetic* phase [5]. In the presence of magnetic field the ground state phase diagram of spin-1 condensate has been investigated both for uniform [8–10] and trapped systems [10, 11]. Similarly, in the absence of external magnetic field, a spin-2 BECs can be in one of the possible three ground state phases: *ferromagnetic*, *anti-ferromagnetic* and *cyclic* [6, 7]. The spin-1 and spin-2 BECs are described by three- and five-component complex order parameters, respectively, thus leading to coupled mean-field Gross-Pitaevskii (GP) equations involving three- and five-component wave functions, which, unlike in a scalar BEC, could be complex in general. A numerical solution of these equations could be cumbersome for both spin-1 [12, 13] and spin-2 [14, 15] BECs. In this paper, we propose simple and useful analytic models for the densities of ground states of quasi-one-dimensional (quasi-1D), circularly-symmetric quasi-two-dimensional (quasi-2D) [16], and spherically-symmetric three-dimensional (3D) spin-1 and spin-2 spinor BECs. Here, we consider nearly-overlapping spatially-symmetric ground states only. Phase-separated spatially-asymmetric pro-files [13] do not appear as ground states and will not be considered.

The two interaction parameters for a spin-1 BEC are $c_0 \propto (a_0 + 2a_2)/3$ and $c_1 \propto (a_2 - a_0)/3$ [5], whereas the three interaction parameters for a spin-2 BEC are $c_0 \propto (4a_2 + 3a_4)/7$, $c_1 \propto (a_4 - a_2)/7$, and $c_2 \propto (7a_0 - 10a_2 + 3a_4)/7$ [6, 7], where a_0, a_2, and a_4 are s-wave scattering lengths in total spin $f_{\text{tot}} = 0, 2$, and 4 channels, respectively. For a ferromagnetic BEC, e.g. for $c_1 < 0$ for a spin-1 BEC, and for $c_1 < 0$ and $c_2 > 20c_1$ for a spin-2 BEC, we find that to a very good approximation the densities for different spin components m_f of the ground-state wave function with magnetization m are multiples of each other. This allows one to replace the coupled GP equation for the ground-state wave function by a single partial differential equation, which we call the decoupled-mode (DM) equation. On the other hand, for an anti-ferromagnetic BEC, e.g. for $c_1 > 0$ for a spin-1 BEC, and for $c_2 < 0$ and $c_2 < 20c_1$ for a spin-2 BEC, we find that the densities, for some of the spin components, of the ground-state wave function with magnetization m are identically zero, thus reducing the original coupled GP equation to a system of two coupled equations for any non-zero magnetization. Similarly, for a cyclic BEC, e.g. for $c_1 > 0$ and $c_2 > 0$ for a spin-2 BEC, the five-component GP equation reduces to a system of two or three coupled equations. These reduced GP equations and the DM equation for the ground state of a spinor BEC in different parameter domains, valid in all spatial dimensions, are solved in the Thomas-Fermi approximation (TFA) (or local-density approximation) to yield simple analytic models for the ground-state densities of spin-1 and spin-2 spinor BECs.

The TFA is applicable when the interaction energy in the GP equation is much larger than the kinetic energy term, so that the latter could be neglected, thus leading to simple analytic formulae for the condensate densities [17]. In a repulsive scalar BEC, applicability of TFA requires that the size of the condensate R is much larger than the oscillator length l_0, i.e. $R/l_0 >> 1$ [18, 19]. The

spatial extent of the BEC in units of l_0 is

$$l_{\mathcal{D}} = \frac{R}{l_0} \sim \left(\frac{Na}{l_0}\right)^{1/(\mathcal{D}+2)}, \qquad (1)$$

where $\mathcal{D} = 1, 2, 3$ is the dimensionality of the space [18, 19]. The criterion is satisfied if the dimensionless parameter $Na/l_0 >> 1$. The ratio Na/l_0 is a measure of the strength of repulsive interaction. For a spinor BEC, the applicability of TFA for m_f component requires that its spatial extent is much larger than l_0.

There have been few studies to include the neglected kinetic energy contribution in the TFA [18, 20]. Earlier, the TFA was used to study the ground state properties of binary condensates [21] and spin dynamics in quasi-1D spin-1 condensate [22]. Spin-orbit-coupled pseudospin-1/2 BECs under rotation have also been theoretically investigated using the TFA [23].

We use the experimentally realizable trapping potential and interaction parameters to illustrate the present analytic models for ground-state densities in different parameter domains. In the case of a spin-1 BEC, the background scattering lengths of ^{87}Rb and ^{23}Na fall in the ferromagnetic [24, 25] and anti-ferromagnetic [26] domains, respectively, and we use these to study the ground state properties. In the case of a spin-2 BEC, we employ ^{23}Na and ^{83}Rb BECs for the illustration. The background scattering lengths of spin-2 ^{23}Na and ^{83}Rb correspond to the anti-ferromagnetic and ferromagnetic phases, respectively [6]. By tuning one of the scattering lengths of ^{23}Na, one can move from anti-ferromagnetic to either ferromagnetic or cyclic phase. Experimentally, such a change of single scattering length can be achieved by exploiting magnetic [27] and optical [28] Feshbach resonance techniques. The results of the analytic models are also validated by a numerical solution of the original mean-field GP equations for quasi-1D and quasi-2D traps.

In Sec. II, we present the full mean-field GP equations for spin-1 and spin-2 BECs and derive the reduced mean-field GP equations for the ground-state wave function in the different parameter domains. By assuming that the component wavefunctions of a ferromagnetic BEC are proportional to each other, which is indeed the case as suggested by numerical simulations, we derive the DM equation. By minimizing the c_1- and c_2-dependent energy terms for the ground-state wave function, we obtain the reduced GP equations in all parameter domains. In Secs. III and IV we obtain the analytic models for spin-1 and spin-2 ground-state BECs, respectively, by employing the TFA to the reduced GP and the DM equations. A comparison of the analytic densities with the numerical densities obtained from the full GP equations leads to a very satisfactory agreement. In Sec. V, we present a summary and concluding remarks. Some of the technical details about the derivation of the DM equation and the reduced GP equations in different parameter domains are presented in Appendix A and B.

II.   REDUCED MEAN-FIELD EQUATIONS

A.   Spin-1 BEC

The coupled GP equations for different spin components $m_f = \pm 1, 0$, for a spin-1 BEC of N atoms of mass M each can be written in dimensionless form as [2]

$$\mu_{\pm 1}\phi_{\pm 1}(\mathbf{x}) = \mathcal{H}\phi_{\pm 1}(\mathbf{x}) + c_0\rho\phi_{\pm 1}(\mathbf{x}) \pm c_1 F_z\phi_{\pm 1}(\mathbf{x})$$
$$+ (c_1/\sqrt{2})F_{\mp}\phi_0(\mathbf{x}), \qquad (2)$$
$$\mu_0\phi_0(\mathbf{x}) = \mathcal{H}\phi_0(\mathbf{x}) + c_0\rho\phi_0(\mathbf{x}) + (c_1/\sqrt{2})[F_-\phi_{-1}(\mathbf{x})$$
$$+ F_+\phi_{+1}(\mathbf{x})], \qquad (3)$$

where

$$F_{\pm} \equiv F_x \pm F_y = \sqrt{2}[\phi_{\pm 1}^*(\mathbf{x})\phi_0(\mathbf{x}) + \phi_0^*(\mathbf{x})\phi_{\mp 1}(\mathbf{x})], \quad (4)$$

$$F_z = \rho_{+1}(\mathbf{x}) - \rho_{-1}(\mathbf{x}), \quad \mathcal{H} = \left[-\frac{1}{2}\nabla^2 + V(\mathbf{x})\right], \quad (5)$$

and the component density $\rho_j = |\phi_j(\mathbf{x})|^2$ with $j = \pm 1, 0$, the total density $\rho = \sum_j \rho_j$, and $\mu_{\pm 1}, \mu_0$ are the respective chemical potentials and * denotes complex conjugate. In 3D, the interaction parameters, Laplacian, and trapping potential are defined as

$$c_0 = \frac{4\pi N(a_0 + 2a_2)}{3l_0}, \ c_1 = \frac{4\pi N(a_2 - a_0)}{3l_0}, \qquad (6)$$

$$\nabla^2 = \frac{\partial^2}{\partial x^2} + \frac{\partial^2}{\partial y^2} + \frac{\partial^2}{\partial z^2}, V(\mathbf{x}) = \frac{x^2 + \beta^2 y^2 + \gamma^2 z^2}{2}, \ (7)$$

with $\mathbf{x} \equiv \{x, y, z\}$. Here $l_0 = \sqrt{\hbar/(M\omega_x)}$, $\beta = \omega_y/\omega_x$, $\gamma = \omega_z/\omega_x$, where $\omega_x, \omega_y, \omega_z$ are the confining trap frequencies in x, y, z directions, respectively. When the trapping frequency along one axis, say ω_z, is much larger than the geometric mean of other two, i.e., $\omega_z \gg \sqrt{\omega_x\omega_y}$, then one can approximate the Eqs. (2) -(3) by quasi two-dimensional (2D) equations which can be obtained by substituting [16]

$$c_0 = \frac{2N\sqrt{2\pi}(a_0 + 2a_2)}{3l_z}, \ c_1 = \frac{2N\sqrt{2\pi}(a_2 - a_0)}{3l_z}, \quad (8)$$

$$\nabla^2 = \frac{\partial^2}{\partial x^2} + \frac{\partial^2}{\partial y^2}, \ V(\mathbf{x}) = \frac{x^2 + \beta^2 y^2}{2}, \ \mathbf{x} \equiv \{x, y\}, \ (9)$$

in Eqs. (2) -(3), here $l_z = \sqrt{\hbar/(M\omega_z)}$. Similarly, if the trapping frequencies along two axes, say y and z, are much larger than the third frequency ω_x, Eqs. (2) -(3) can be approximated by quasi-1D equations which can be obtained by substituting

$$c_0 = \frac{2N(a_0 + 2a_2)l_0}{3l_{yz}^2}, \ c_1 = \frac{2N(a_2 - a_0)l_0}{3l_{yz}^2}, \quad (10)$$

$$\nabla^2 = \frac{\partial^2}{\partial x^2}, \ V(\mathbf{x}) = \frac{x^2}{2}, \ \mathbf{x} \equiv x, \qquad (11)$$

where $l_{yz} = \sqrt{\hbar/(M\omega_{yz})}$ and $\omega_{yz} = \sqrt{\omega_y\omega_z}$. Here length is measured in units of l_0, density in units of $l_0^{-\mathcal{D}}$ and

chemical potential in units of $\hbar\omega_x$, where $\mathcal{D} = 1, 2, 3$ is the dimensionality of space. The total density is normalized to unity $\int d\mathbf{x}\rho(\mathbf{x}) = 1$. The volume element $d\mathbf{x} = 2dX$ in 1D, $2\pi X dX$ in 2D with circular symmetry, and $4\pi X^2 dX$ in 3D with spherical symmetry, where $X = |\mathbf{x}|$ is the length of the vector $\mathbf{x}$. In this paper, we consider isotropic 3D and isotropic quasi-2D traps, i.e., $\beta = \gamma = 1$ for 3D traps and $\beta = 1 \ll \gamma$ for quasi-2D traps.

Numerical calculation for the ground-state densities of a of a ferromagnetic BEC ($c_1 < 0$) has revealed that the component densities are essentially multiples of each other. This opens the possibility of writing a single decoupled mode (DM) equation for the wave-function $\phi_{\rm DM}$ for the ferromagnetic BEC and obtain the component wave functions as multiples of this wave function according to

$$\phi_j(\mathbf{x}) = \alpha_j\phi_{\rm DM}(\mathbf{x}), \quad j = \pm 1, 0, \tag{12}$$

where α_j's, in general, are complex numbers. The conditions (12) when substituted in Eqs. (2) and (3) lead to three different equations for the same wave function $\phi_{\rm DM}$. A consistency requirement on these three equations leads to the single decoupled-mode (DM) equation for the wave function $\phi_{\rm DM}$:

$$\mu\phi_{\rm DM}(\mathbf{x}) = \left[-\frac{1}{2}\nabla^2 + V(\mathbf{x}) + C\phi_{\rm DM}^2(\mathbf{x})\right]\phi_{\rm DM}(\mathbf{x}), \tag{13}$$

with $C \equiv \mathcal{C}_I = c_0 + c_1$ and normalization $\int \rho_{\rm DM}(\mathbf{x})d\mathbf{x} = 1$, provided that

$$|\alpha_{\pm 1}| = \frac{1 \pm m}{2}, \quad |\alpha_0| = \frac{\sqrt{1 - m^2}}{\sqrt{2}}, \tag{14}$$

$$m \equiv \int d\mathbf{x}[\rho_{+1} - \rho_{-1}] = |\alpha_{+1}|^2 - |\alpha_{-1}|^2, \tag{15}$$

where m is the magnetization. An equation similar to Eq. (13) with $C = c_0 \sim (a_0 + 2a_2)/3$, known as the single-mode approximation (SMA) [29], was obtained before as an approximation to Eqs. (2)-(3). The component densities were then obtained using Eq. (14). In the DM model we have a different $C \equiv \mathcal{C}_I = (c_0 + c_1) \sim a_2$, which is independent of a_0. Equation (13) was previously obtained by Yi et al. [30] as an improvement over the SMA. The breakdown of the single-mode approximation for trapped spin-1 condensates in the presence of magnetic field has also been theoretically investigated [10].

Provided that ansatz (12) holds, distribution (14) can be obtained independently from a consideration of c_1-dependent energy minimization for a ferromagnetic BEC as shown in Appendix A. The DM equation is very useful for finding the ground state of a ferromagnetic BEC where all density components are non-zero and this procedure can also be readily generalized to higher-spin cases as shown in Sec. II B for a spin-2 ferromagnetic BEC.

For the ground-state of an anti-ferromagnetic BEC ($c_1 > 0$) with non-zero magnetization, energy minimization requires that $\phi_0(\mathbf{x}) = 0$, viz. Appendix A. Then the normalization and magnetization conditions yield

$$\int \rho_{\pm 1}d\mathbf{x} = \frac{1 \pm m}{2}, \quad \rho_0 = 0. \tag{16}$$

For $m = 0$, besides the aforementioned state, there is another degenerate state where all the atoms are in $m_f = 0$ component, i.e. $\rho_{\pm 1} = 0$ and $\int \rho_0 d\mathbf{x} = 1$. Unlike in a ferromagnetic BEC, ansatz (12) does not hold for an anti-ferromagnetic BEC for a non-zero magnetization m where different components occupy different spatial extensions. On the other hand, for $m = 0$, SMA becomes exact in this phase [30], as the c_1-dependent term vanishes.

We will derive the analytic model for a ferromagnetic BEC using the TFA to the DM equation (13), whereas for an anti-ferromagnetic BEC we rely on the TFA to the GP equation (2) with $\phi_0(\mathbf{x}) = 0$ for the same.

B. Spin-2 BEC

The dimensionless coupled GP equations for different spin components $m_f = \pm 2, \pm 1, 0$, for a spin-2 BEC can be written as [2]

$$\mu_{\pm 2}\phi_{\pm 2}(\mathbf{x}) = \mathcal{H}\phi_{\pm 2}(\mathbf{x}) + c_0\rho\phi_{\pm 2}(\mathbf{x}) + (c_2/\sqrt{5})\Theta\phi_{\mp 2}^*(\mathbf{x}) + c_1\left[F_{\mp}\phi_{\pm 1}(\mathbf{x}) \pm 2F_z\phi_{\pm 2}(\mathbf{x})\right], \tag{17}$$

$$\mu_{\pm 1}\phi_{\pm 1}(\mathbf{x}) = \mathcal{H}\phi_{\pm 1}(\mathbf{x}) + c_0\rho\phi_{\pm 1}(\mathbf{x}) - (c_2/\sqrt{5})\Theta\phi_{\mp 1}^*(\mathbf{x}) + c_1\left[\sqrt{3/2}F_{\mp}\phi_0(\mathbf{x}) + F_{\pm}\phi_{\pm 2}(\mathbf{x}) \pm F_z\phi_{\pm 1}(\mathbf{x})\right], \tag{18}$$

$$\mu_0\phi_0(\mathbf{x}) = \mathcal{H}\phi_0(\mathbf{x}) + c_0\rho\phi_0(\mathbf{x}) + (c_2/\sqrt{5})\Theta\phi_0^*(\mathbf{x}) + c_1\sqrt{3/2}\left[F_-\phi_{-1}(\mathbf{x}) + F_+\phi_{+1}(\mathbf{x})\right], \tag{19}$$

where

$$F_+ = F_-^* = 2(\phi_{+2}^*\phi_{+1} + \phi_{-1}^*\phi_{-2}) + \sqrt{6}(\phi_{+1}^*\phi_0 + \phi_0^*\phi_{-1}), \tag{20}$$

$$F_z = 2(|\phi_{+2}|^2 - |\phi_{-2}|^2) + |\phi_{+1}|^2 - |\phi_{-1}|^2, \tag{21}$$

$$\Theta = \frac{2\phi_{+2}\phi_{-2} - 2\phi_{+1}\phi_{-1} + \phi_0^2}{\sqrt{5}}. \tag{22}$$

Here the interaction parameters $c_0 = 4\pi N(4a_2 + 3a_4)/(7l_0), c_1 = 4\pi N(a_4 - a_2)/(7l_0), c_2 = 4\pi N(7a_0 - 10a_2 + 3a_4)/(7l_0)$, $\mu_{\pm 2}, \mu_{\pm 1}$, and μ_0 are the respective chemical potentials. All repeated variables have the same meaning as in the spin-1 case. The total density ρ is again normalized to unity. As in the spin-1 case, GP equations in quasi-2D traps can be obtained by using Eqs. (9) and substituting $c_0 = 2N\sqrt{2\pi}(4a_2 + 3a_4)/(7l_z), c_1 = 2N\sqrt{2\pi}(a_4 - a_2)/(7l_z), c_2 = 2N\sqrt{2\pi}(7a_0 - 10a_2 + 3a_4)/(7l_z)$ in Eqs. (17)-(19). Similarly, GP equations in quasi-1D traps can be obtained by using Eqs. (11) and substituting $c_0 = 2N(4a_2 + 3a_4)l_0/(7l_{yz}^2), c_1 = 2N(a_4 - a_2)l_0/(7l_{yz}^2), c_2 = 2N(7a_0 - 10a_2 + 3a_4)l_0/(7l_{yz}^2)$ in Eqs. (17)-(19).

In the DM, for a ferromagnetic BEC ($c_1 < 0, c_2 > 20c_1$) with all non-zero component densities, if we substitute the *ansatz*

$$\phi_j = \alpha_j \phi_{\text{DM}}, \quad j = \pm 2, \pm 1, 0, \qquad (23)$$

in Eqs. (17), (18), and (19), we obtain five independent equations for ϕ_{DM}. A consistency requirement among these five equations for the c_1-dependent terms leads to the DM equation (13) with $C \equiv \mathcal{C}_{II} = (c_0 + 4c_1)$, provided that

$$|\alpha_{\pm 2}| = \frac{(2 \pm m)^2}{16}, \qquad (24)$$

$$|\alpha_{\pm 1}| = \frac{\sqrt{4 - m^2}(2 \pm m)}{8}, \qquad (25)$$

$$|\alpha_0| = \frac{1}{8}\sqrt{\frac{3}{2}}\left(4 - m^2\right), \qquad (26)$$

with magnetization and normalization conditions

$$m \equiv \int d\mathbf{x}[2(\rho_{+2} - \rho_{-2}) + (\rho_{+1} - \rho_{-1})], \qquad (27)$$

$$= 2(|\alpha_{+2}|^2 - |\alpha_{-2}|^2) + (|\alpha_{+1}|^2 - |\alpha_{-1}|^2), \qquad (28)$$

$$1 = |\alpha_{+2}|^2 + |\alpha_{-2}|^2 + |\alpha_{+1}|^2 + |\alpha_{-1}|^2 + |\alpha_0|^2. \, (29)$$

In the DM model for a spin-2 BEC $C \equiv \mathcal{C}_{II} \sim a_4$ is independent of the scattering lengths a_0 and a_2, with a_4 playing the role of scattering length in an equivalent scalar BEC. With the coefficients $\alpha_{\pm 2}, \alpha_{\pm 1}, \alpha_0$ given by Eqs. (24)-(26) the coefficient Θ of Eq. (22) is identically equal to 0. The condition $\Theta = 0$ for the ground state makes the GP equations (17)-(19) simpler and independent of c_2. Consequently, the DM equation (13) becomes an exact equation for the ground state wave function provided Eq. (23) holds, e.g. the component wave functions are multiples of each other. Our numerical calculations show that the condition (23) holds for all magnetization to a very high degree of accuracy.

The coefficients $\alpha_{\pm 2}, \alpha_{\pm 1}, \alpha_0$ can also be obtained from a minimization of energy along with condition (23), for a ferromagnetic ground state with $c_1 < 0$ and $c_2 > 20c_1$. An explicit account of the derivation of the coefficients $\alpha_{\pm 2}, \alpha_{\pm 1}, \alpha_0$, from an energy minimization for a ferromagnetic spin-2 BEC is given in Appendix B.

For an anti-ferromagnetic BEC ($c_2 < 0, c_2 < 20c_1$) for any non-zero magnetization m numerical studies show that $\phi_{\pm 1}(\mathbf{x}) = \phi_0(\mathbf{x}) = 0$ for the ground state. This can also be obtained from energetic consideration as shown in Appendix B. The magnetization and normalization conditions (27) and (29) then yield

$$\int \rho_{\pm 2} d\mathbf{x} = \frac{2 \pm m}{4}, \qquad (30)$$

Energy consideration establishes that a cyclic BEC ($c_1 > 0, c_2 > 0$) has two degenerate ground states for all non-zero magnetization m with $(i)\phi_{+1}(\mathbf{x}) = \phi_0(\mathbf{x}) = \phi_{-2}(\mathbf{x}) = 0$, or with $(ii)\phi_{\pm 1}(\mathbf{x}) = 0$, viz. Appendix B.
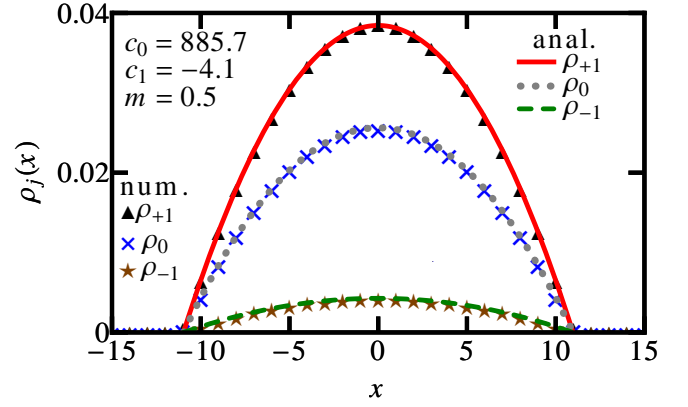

FIG. 1: (Color online) Analytic (anal.) and numerical (num.) densities of a spin-1 quasi-1D ferromagnetic ^{87}Rb BEC. The number of atoms, scattering lengths and oscillator lengths are, respectively, $N = 10,000$, $a_0 = 101.8a_B$, $a_2 = 100.4a_B$ [24], $l_0 = 2.41\mu$m, $l_{yz} = 0.54\mu$m, here a_B is Bohr radius.

Consequently, the magnetization and normalization conditions (27) and (29) lead for these two states

$$(i) \int d\mathbf{x}\rho_{+2} = \frac{1 + m}{3}, \quad \int d\mathbf{x}\rho_{-1} = \frac{2 - m}{3}, \qquad (31)$$

$$(ii) \int d\mathbf{x}\rho_{\pm 2} = \left(\frac{2 \pm m}{4}\right)^2, \quad \int d\mathbf{x}\rho_0 = \frac{4 - m^2}{8}. \, (32)$$

For both anti-ferromagnetic and cyclic BECs we will derive the analytic models directly from the TFA to the GP equations (17)-(19) and not from the DM, whereas for a ferromagnetic BEC we will rely on the TFA to the DM equation (13) with $C = (c_0 + 4c_1)$.

III. ANALYTIC MODEL FOR SPIN-1 BEC

A. Ferromagnetic BEC

We derive the analytic model for the ground-state density of a spin-1 BEC using the TFA to the DM equation (13) with component densities given by Eq. (14). In the TFA the kinetic energy term in Eq. (13) is neglected, which is reasonable for a moderate to large positive nonlinear terms, and the BEC density is calculated by equating the "Hamiltonian" to the chemical potential by

$$\mu = [X^2/2 + C\rho_{\text{DM}}], \quad C \equiv \mathcal{C}_I = c_0 + c_1, \qquad (33)$$

thus leading to the TFA density

$$\rho_{\text{DM}}(X) = (l_{\mathcal{D}}^2 - X^2)/(2\mathcal{C}_I), \quad X \leq l_{\mathcal{D}} = \sqrt{2\mu}. \qquad (34)$$

Imposing the condition of normalization $\int \rho_{\text{DM}}(X)d\mathbf{x} = 1$, we obtain, in 1D, 2D, and 3D, respectively $l_{\mathcal{D}} = (3\mathcal{C}_I/2)^{1/3}, (4\mathcal{C}_I/\pi)^{1/4}$ and $(15\mathcal{C}_I/4\pi)^{1/5}$, provided $\mathcal{C}_I >$
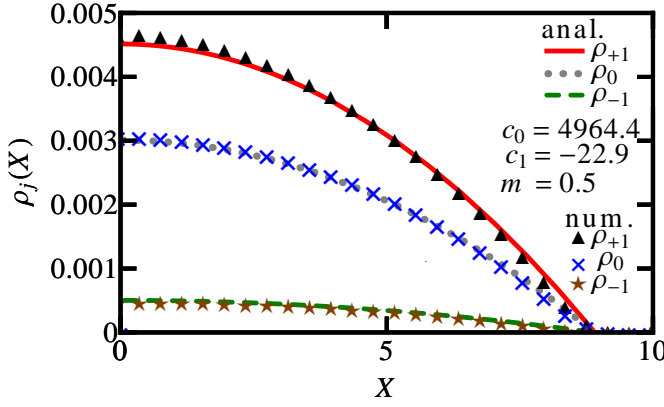
FIG. 2: (Color online) Analytic (anal.) and numerical (num.) densities of a spin-1 quasi-2D ferromagnetic ^{87}Rb BEC. The number of atoms, scattering lengths and oscillator lengths are, respectively, $N = 100,000$, $a_0 = 101.8a_B$, $a_2 = 100.4a_B$ [24], $l_0 = 2.41\mu$m, $l_z = 0.54\mu$m, here a_B is Bohr radius.

FIG. 3: (Color online) Analytic (anal.) and numerical (num.) densities of a spin-1 quasi-1D anti-ferromagnetic ^{23}Na BEC. The number of atoms, scattering lengths and oscillator lengths are, respectively, $N = 10,000$; $a_0 = 47.36a_B$, $a_2 = 52.98a_B$ [3]; $l_0 = 4.69\mu$m, $l_{yz} = 1.05\mu$m.

0. The component densities are calculated using Eqs. (12) and (14). The analytic densities for a quasi-1D spin-1 ferromagnetic ^{87}Rb BEC are shown in Fig. 1 along with the numerical solution of the full coupled GP equations (2)-(3). The same for a quasi-2D spin-1 ferromagnetic ^{87}Rb BEC is shown in Fig. 2. All numerical calculations are performed using the split-step Crank-Nicolson scheme [31] with space and time steps 0.025 and 0.00005, respectively.

In the DM model $\mathcal{C}_I \sim a_2$ plays the same role as the scattering length a in a scalar BEC in Eq. (1). Hence in this case the condition of validity of the TFA will be $Na_2/l_0 >> 1$.

B. Anti-ferromagnetic BEC

In this case, the analytic model is derived by applying TFA directly to the GP equation (2) with $\phi_0(\mathbf{x}) = 0$. For a non-zero magnetization ($0 < m < 1$), the $m_f = +1$ component accommodates more atoms and its spatial extension $l_{\mathcal{D}(+1)}$ is larger than the same of the the $m_f = -1$ component with spatial extension $l_{\mathcal{D}(-1)}$. Hence for $l_{\mathcal{D}(+1)} > x > l_{\mathcal{D}(-1)}$, $\phi_{-1}(\mathbf{x}) = 0$ and the coupled GP equation (2) for $\phi_{\pm 1}(\mathbf{x})$ reduces to a single equation for $\phi_{+1}(\mathbf{x})$. In the TFA, the kinetic energy terms in the GP equation (2) are neglected and the densities are calculated by equating the Hamiltonian to the respective chemical potentials:

$$\mu_{\pm 1} = \left[X^2/2 + c_0\rho\right] + c_1(\rho_{\pm 1} - \rho_{\mp 1}), \quad X \leq l_{\mathcal{D}(-1)},$$

(35)

$$\mu_{+1} = \left[X^2/2 + \mathcal{C}_I \rho_{+1}\right], \quad l_{\mathcal{D}(+1)} \geq X \geq l_{\mathcal{D}(-1)},$$
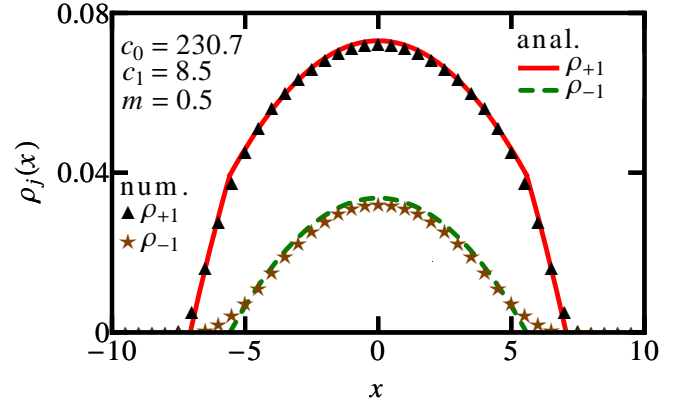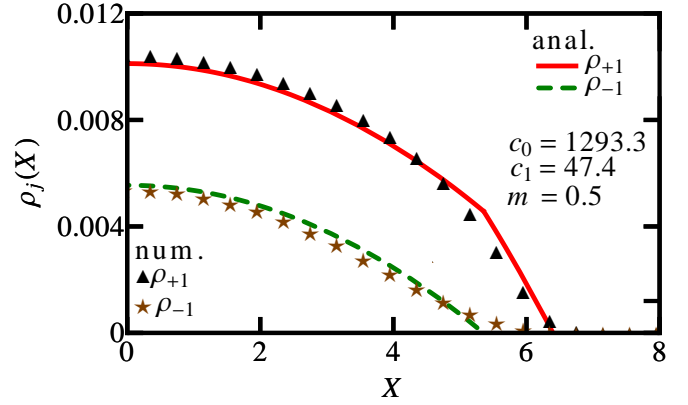
(36)

FIG. 4: (Color online) Analytic (anal.) and numerical (num.) densities of a spin-1 quasi-2D anti-ferromagnetic ^{23}Na BEC. The number of atoms, scattering lengths and oscillator lengths are, respectively, $N = 100,000$; $a_0 = 47.36a_B$, $a_2 = 52.98a_B$ [3]; $l_0 = 4.69\mu$m, $l_z = 1.05\mu$m.

subject to normalization (16). In the domain $l_{\mathcal{D}(+1)} \geq X \geq l_{\mathcal{D}(-1)}$, Eq. (36) has the solution

$$\rho_{+1}(X) = \frac{l_{\mathcal{D}(+1)}^2 - X^2}{2\mathcal{C}_I}, \quad l_{\mathcal{D}(+1)} \geq X \geq l_{\mathcal{D}(-1)},$$

(37)

$$\mu_{+1} = l_{\mathcal{D}(+1)}^2/2.$$

(38)

In the overlap region $X \leq l_{\mathcal{D}(-1)}$, coupled equations (35) have the solution

$$\rho_{\pm 1}(X) = \frac{c_0(\mu_{\pm 1} - \mu_{\mp 1}) + c_1(\mu_{+1} + \mu_{-1} - X^2)}{4c_0c_1}.$$

(39)

The condition $\rho_{-1}(l_{\mathcal{D}(-1)}) = 0$ leads to

$$\mu_{-1} = \frac{(c_0 - c_1)l_{\mathcal{D}(+1)}^2 + 2c_1 l_{\mathcal{D}(-1)}^2}{2\mathcal{C}_I}. \tag{40}$$

Substituting Eqs. (38) and (40) in Eq. (39), we obtain

$$\rho_{+1}(X) = \frac{2c_0 l_{\mathcal{D}(+1)}^2 + (c_1 - c_0)l_{\mathcal{D}(-1)}^2 - \mathcal{C}_I X^2}{4c_0 \mathcal{C}_I}, \quad X \leq l_{\mathcal{D}(-1)} \tag{41}$$

$$\rho_{-1}(X) = \frac{(l_{\mathcal{D}(-1)}^2 - X^2)}{4c_0}, \quad X \leq l_{\mathcal{D}(-1)}. \tag{42}$$

The normalization condition (16) for $\rho_{\pm 1}(X)$ leads to

$$l_{\mathcal{D}(-1)} = l_{\mathcal{D}}[c_0(1 - m)/\mathcal{C}_I]^{1/(2+\mathcal{D})}, \tag{43}$$

$$l_{\mathcal{D}(+1)} = l_{\mathcal{D}}[(c_0 + c_1 m)/\mathcal{C}_I]^{1/(2+\mathcal{D})}. \tag{44}$$

The densities (37), (41) and (42) with extensions given by Eqs. (43)-(44) constitute the analytic model in this case.

These analytic densities for a spin-1 quasi-1D anti-ferromagnetic ^{23}Na BEC are shown in Fig. 3 along with the numerical solution of the full coupled GP equations (2)-(3). The same for a spin-1 quasi-2D anti-ferromagnetic ^{23}Na BEC are shown in Fig. 4. Comparing Eq. (1) with Eqs. (43)-(44), the conditions for the validity of TFA in this case are

$$\frac{N(a_0 + 2a_2)(1 - m)}{3l_0} >> 1, \tag{45}$$

$$\frac{N[a_0 + 2a_2 + (a_2 - a_0)m]}{3l_0} >> 1, \tag{46}$$

for $m_f = -1$ and $m_f = +1$ component, respectively. The terms on the left side of Eqs. (45) and (46) are the measure of the repulsive interactions in $m_f = -1$ and $m_f = +1$ components, respectively.

For magnetization $m = 0$ there is another degenerate ground state where all atoms are in the $m_f = 0$ component [2]. In that case the spin-1 GP equation reduces to the DM equation (33) with $\mathcal{C}_I = c_0$ and $\rho_0(X) = \rho_{DM}(X)$ of Eq. (34). From Eqs. (45)-(46), the simple criterion for the validity of TFA in this case is $N(a_0 + 2a_2)/(3l_0) >> 1$, which is consistent with the fact that for $m = 0$, c_1 term does not contribute to the energy of the system.

The TF analysis shows that the spatial extents of the components are different for an anti-ferromagnetic BEC for any non-zero magnetization, viz. Eqs. (43)-(44), which is also manifested by different chemical potentials, viz. Eqs. (38) and (40), whereas these are the same for a ferromagnetic BEC. Thus, in the domain $l_{\mathcal{D}(-1)} \leq X < l_{\mathcal{D}(+1)}$ only component $m_f = +1$ survives for the anti-ferromagnetic BEC effectively separating this component from mixed phase in the $X < l_{\mathcal{D}(-1)}$ domain. The different spatial extents of the components for an anti-ferromagnetic BEC also imply that SMA is not valid

in general except for $m = 0$, when $l_{\mathcal{D}(\pm 1)}$ of Eqs. (43)-(44) become equal. The ground states shown in Figs. 3 and 4 preserve the symmetry of the trapping potential. These symmetric profiles minimize c_1-dependent interaction energy [30]

$$E_A = \frac{c_1}{2} \int \left[(\rho_{+1} - \rho_{-1})^2 + 2\rho_0(\rho_{+1} + \rho_{-1}) - 4\sqrt{\rho_{+1}\rho_{-1}}\rho_0 \right] d\mathbf{x}. \tag{47}$$

The asymmetric states, where the two phase-separated components lie side by side [13], do not minimize E_A in addition to having more potential-energy contribution. Hence, they do not emerge as the ground states in trapped spinor condensates. The asymmetric states can emerge as the ground state in the presence of Zeeman energy [2, 11] or spin-orbit coupling [13, 15] which we do not include in the Hamiltonian.

IV. ANALYTIC MODEL FOR SPIN-2 BEC

A. Ferromagnetic BEC

In this case, the component densities are given by the DM equation (23) along with distributions (24)-(26) and the analytic model is derived from the TFA to the DM equation (13). Following the procedure of Sec. III A for a spin-1 ferromagnetic BEC, the TFA densities are again given by Eq. (34), but now with $C \equiv \mathcal{C}_{II} = c_0 + 4c_1$. The component densities are then obtained using Eqs. (24)-(26). These analytic densities for a quasi-1D spin-2 ferromagnetic ^{23}Na and ^{83}Rb BECs are shown in Figs. 5(a) and (b), respectively, together with the numerical densities from the full coupled GP equations (17)-(19).

In the DM model $\mathcal{C}_{II} \sim a_4$ plays the same role as the scattering length a in a scalar BEC in Eq. (1). Hence in this case the condition of validity of the TFA will be $Na_4/l_0 >> 1$.

B. Anti-ferromagnetic BEC

The analytic model here is obtained from the TFA to the GP equation (17) involving only $\phi_{\pm 2}(\mathbf{x})$ subject to $\phi_0(\mathbf{x}) = \phi_{\pm 1}(\mathbf{x}) = 0$ with normalization condition (30). After neglecting the kinetic energy terms in the GP equation (17) the corresponding TFA densities are given by

$$\mu_{\pm 2} = X^2/2 + c_0\rho \pm 4c_1(\rho_{+2} - \rho_{-2}) + \frac{2c_2\rho_{\mp 2}}{5}, \tag{48}$$

For a non-zero magnetization $0 < m \leq 2$, the $m_f = +2$ component extends to a larger domain $(X < l_{\mathcal{D}(+2)})$ than the $m_f = -2$ component with a smaller extension $(X < l_{\mathcal{D}(-2)}, l_{\mathcal{D}(+2)} > l_{\mathcal{D}(-2)})$. Following the procedure presented in Sec. III B for a spin-1 anti-ferromagnetic
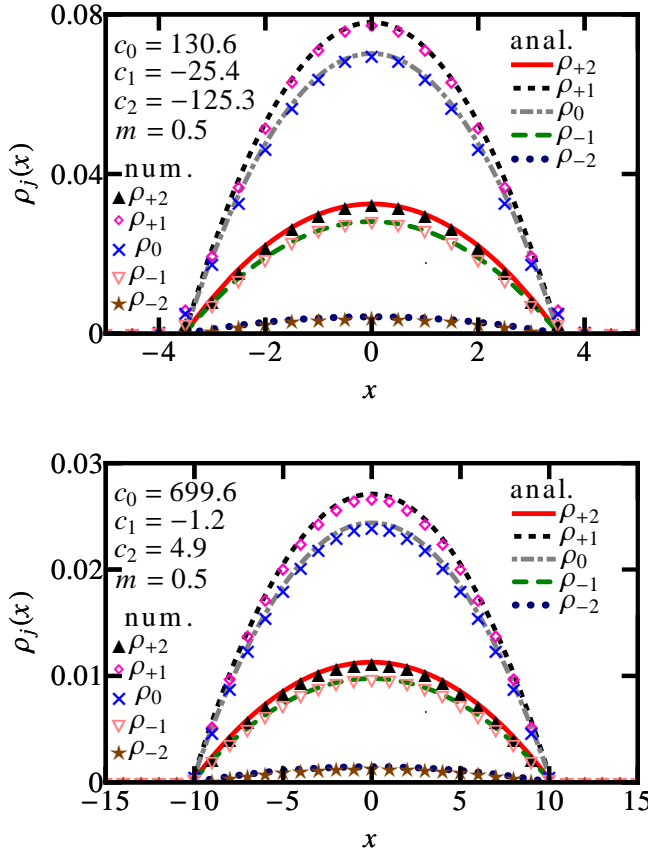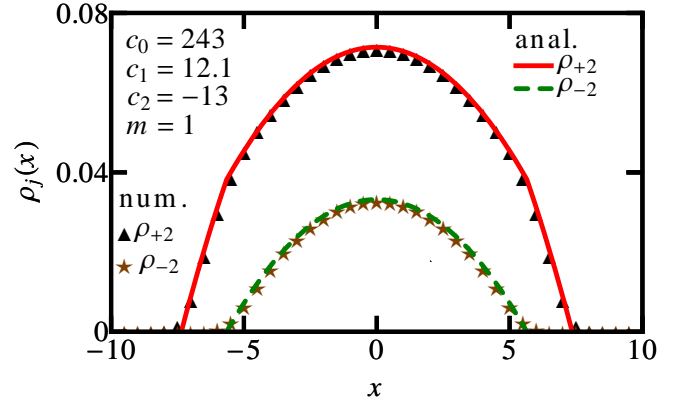
FIG. 6: (Color online) Analytic (anal.) and numerical (num.) densities of a spin-2 quasi-1D anti-ferromagnetic ^{23}Na BEC. The number of atoms, scattering lengths and oscillator lengths are, respectively, $N = 10,000$; $a_0 = 34.9a_B$, $a_2 = 45.8a_B$, $a_4 = 64.5a_B$ [6] ; $l_0 = 4.69\mu$m, $l_{yz} = 1.05\mu$m.

where $\mathcal{B} = (5c_0 + c_2)(2 - m)$. The analytic TFA densities of the spin components $m_f = \pm 2$ are given by

$$\rho_{+2}(X) = \frac{20c_1\left(l_{\mathcal{D}(-2)}^2 - X^2\right) + 2c_2\left(l_{\mathcal{D}(+2)}^2 - l_{\mathcal{D}(-2)}^2\right)}{4\mathcal{C}_{II}(5c_0 + c_2)}$$
$$+ \frac{5c_0\left(2l_{\mathcal{D}(+2)}^2 - l_{\mathcal{D}(-2)}^2 - X^2\right)}{4\mathcal{C}_{II}(5c_0 + c_2)}, \quad X \leq l_{\mathcal{D}(-2)}, \tag{51}$$

$$\rho_{+2}(X) = \frac{l_{\mathcal{D}(+2)}^2 - X^2}{2\mathcal{C}_{II}}, \quad l_{\mathcal{D}(+2)} \geq X \geq l_{\mathcal{D}(-2)}, \tag{52}$$

$$\rho_{-2}(X) = \frac{5\left(l_{\mathcal{D}(-2)}^2 - X^2\right)}{4(5c_0 + c_2)}, \quad X \leq l_{\mathcal{D}(-2)}, \tag{53}$$

with the extensions $l_{\pm 2}$ given by Eqs. (49) and (50). The analytic and numerical densities for a quasi-1D spin-2 anti-ferromagnetic ^{23}Na BEC are compared in Fig. 6. Again, in this case, phase-separated asymmetric profiles do not emerge as ground states due to more energy contribution from c_2-dependent energy term in addition to more potential energy as compared to symmetric profiles.

Comparing Eq. (1) with Eqs. (49)-(50), the conditions for the validity of TFA in this case are

$$\frac{N[c_{0a} + 2c_{1a}m + c_{2a}(2 - m)/10]}{7l_0} >> 1, \tag{54}$$

$$\frac{N[(c_{0a} + c_{2a}/5)(1 - m/2)]}{7l_0} >> 1, \tag{55}$$

for $m_f = +2$ and $m_f = -2$ components, respectively, where $c_{0a} = 4a_2 + 3a_4$, $c_{1a} = a_4 - a_2$, and $c_{2a} = 7a_0 - 10a_2 + 3a_4$.

For $m = 0$ there is another degenerate ground state with the all the atoms in the $m_f = 0$ component [3]. In

FIG. 5: (Color online) (a) and (b) show analytic (anal.) and numerical (num.) densities of quasi-1D spin-2 ferromagnetic ^{23}Na and ^{83}Rb BECs, respectively. For ^{23}Na, the number of atoms, scattering lengths and oscillator lengths are, respectively, $N = 10,000$, $a_0 = 34.9a_B$, $a_2 = 45.8a_B$, $a_4 = 6.45a_B$, [6] $l_0 = 4.69\mu$m, $l_{yz} = 1.05\mu$m, here a_B is Bohr radius. The experimental value of $a_4(= 64.5a_B)$ has been modified to access the ferromagnetic phase of ^{23}Na (using a Feshbach resonance) from the natural anti-ferromagnetic phase. For ^{83}Rb, the corresponding parameters are $N = 10,000$, $a_0 = 83.0a_B$, $a_2 = 82.0a_B$, $a_4 = 81.0a_B$, [6] $l_0 = 2.47\mu$m, $l_{yz} = 0.55\mu$m.

BEC, one can calculate $l_{\mathcal{D}(+2)}$ in 1D, 2D and 3D, respectively, as

$$l_{1(+2)} = \frac{[3\mathcal{A}]^{1/3}}{20^{1/3}}, \quad l_{2(+2)} = \frac{[2\mathcal{A}]^{1/4}}{(5\pi)^{1/4}}, \quad l_{3(+2)} = \frac{[3\mathcal{A}]^{1/5}}{(8\pi)^{1/5}}, \tag{49}$$

where $\mathcal{A} = (10c_0 + 2c_2 + 20c_1m - c_2m)$. Similarly, $l_{\mathcal{D}(-2)}$ in 1D, 2D and 3D, respectively, are

$$l_{1(-2)} = \frac{[3\mathcal{B}]^{1/3}}{20^{1/3}}, \quad l_{2(-2)} = \frac{[2\mathcal{B}]^{1/4}}{(5\pi)^{1/4}}, \quad l_{3(-2)} = \frac{[3\mathcal{B}]^{1/5}}{(8\pi)^{1/5}}, \tag{50}$$

this case the GP equation reduces to the DM equation (33) with $\mathcal{C}_{II} = (c_0 + c_2/5)$ and $\rho_0(X) = \rho_{DM}(X)$ of (34). A superposition of this solution and the solution corresponding to Eq. (48) with $m = 0$ will also be a degenerate solution. The simpler criterion for the validity of TFA in this case is $N[(7a_0 + 10a_2 + 18a_4)/5]/(7l_0) \gg 1$, which is consistent with Eqs. (54) and (55) with $m = 0$.

C. Cyclic BEC

In this case, there are two degenerate ground states for all magnetization m with non-zero component densities given by Eqs. (31) and (32), respectively. The analytic models will be obtained in these two cases from the TFA to the GP equations (17)-(19).

The former distribution (31) involves only two non-zero components in the GP equation. After neglecting the kinetic energy terms in the GP equations (17)-(19), the TFA densities for the non-zero spin components $m_f = +2$ and $m_f = -1$ are described by

$$\mu_{+2} = X^2/2 + c_0\rho + 2c_1(2\rho_{+2} - \rho_{-1}), \quad (56)$$

$$\mu_{-1} = X^2/2 + c_0\rho - c_1(2\rho_{+2} - \rho_{-1}). \quad (57)$$

For a non-zero magnetization $(2 > m > 0)$ the $m_f = +2$ component has a larger spatial extension $(l_{\mathcal{D}(+2)})$ than the $m_f = -1$ component with a smaller spatial extension $(\pm l_{\mathcal{D}(-1)}, l_{\mathcal{D}(+2)} > l_{\mathcal{D}(-1)})$. Following the procedure discussed for a spin-1 anti-ferromagnetic BEC in Sec. III B,
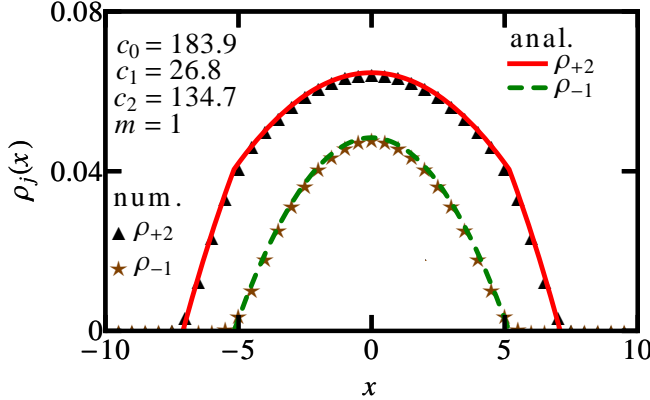

FIG. 7: (Color online) Analytic (anal.) and numerical (num.) densities of a spin-2 quasi-1D cyclic ^{23}Na BEC. The number of atoms, scattering lengths and oscillator lengths are, respectively, $N = 10,000$, $a_0 = 34.9a_B$, $a_2 = 22.9a_B$, $a_4 = 64.5a_B$ [6], $l_0 = 4.69\mu m$, $l_{yz} = 1.05\mu m$. The experimental value of $a_2 (= 45.8a_B)$ has been modified to access the cyclic phase of ^{23}Na (using a Feshbach resonance) from its natural anti-ferromagnetic phase.
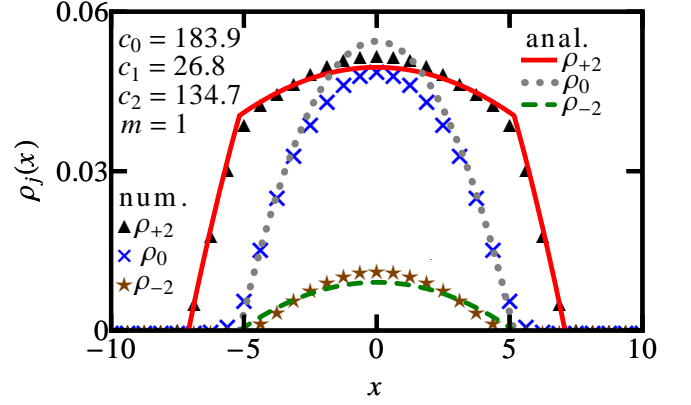

FIG. 8: (Color online) Analytic (anal.) and numerical (num.) densities of a spin-2 quasi-1D ^{23}Na cyclic BEC. All parameters are the same as in Fig. 7.

one obtains

$$l_{\mathcal{D}(+2)} = l_{\mathcal{D}}[(c_0 + 2c_1m)/\mathcal{C}_I]^{1/(2+\mathcal{D})}, \quad (58)$$

$$l_{\mathcal{D}(-1)} = l_{\mathcal{D}}[c_0(2 - m)/2\mathcal{C}_I]^{1/(2+\mathcal{D})}. \quad (59)$$

The normalized densities are given by

$$\rho_{-1}(X) = \frac{(l_{\mathcal{D}(-1)}^2 - X^2)}{3c_0}, \quad X \leq l_{\mathcal{D}(-1)}, \quad (60)$$

$$\rho_{+2}(X) = \frac{3c_0 l_{\mathcal{D}(+2)}^2 - 2(c_0 - 2c_1)l_{\mathcal{D}(-1)}^2 - \mathcal{C}_{II}X^2}{6c_0\mathcal{C}_{II}}, X \leq l_{\mathcal{D}(-1)} \quad (61)$$

$$= \frac{l_{\mathcal{D}(+2)}^2 - X^2}{2\mathcal{C}_{II}}. \quad l_{\mathcal{D}(-1)} \leq X \leq l_{\mathcal{D}(+2)}, \quad (62)$$

Equations (60)-(62) together with extensions given by Eqs. (58)-(59) are the analytic densities in this case. The analytic and numerical densities for a quasi-1D spin-2 cyclic ^{23}Na BEC are shown in Fig. 7. For $m = 0$, SMA becomes exact for the cyclic phase of spin-2 condensate, as the c_1 and c_2-dependent terms in Eqs. (56)-(57) vanish.

Comparing Eq. (1) and Eqs. (58)-(59), the conditions for the validity of TFA in this case are

$$\frac{N[4a_2 + 3a_4 + 2(a_4 - a_2)m]}{7l_0} \gg 1, \quad (63)$$

$$\frac{N[4a_2 + 3a_4(1 - m/2)]}{7l_0} \gg 1, \quad (64)$$

for $m_f = +2$ and $m_f = -1$ components, respectively. For $m = 0$ the simple criterion for the validity of TFA is $N(4a_2 + 3a_4)/(7l_0) \gg 1$, which is consistent with fact that only spin-independent non-linearity (c_0 dependent term) contributes to the energy of the system.

Similarly, for the latter distribution (32), after neglecting the kinetic energy terms in the GP equations (17)-

(19), the TFA densities are given by

$$\mu_{\pm 2} = X^2/2 + c_0\rho \pm 4c_1(\rho_{+2} - \rho_{-2}), \quad (65)$$

$$\mu_0 = X^2/2 + c_0\rho. \quad (66)$$

This set of equations for $\rho_{\pm 2}$ and ρ_0 is overcomplete and does not determine the densities. However, if we assume, consistent with Eq. (32), that

$$\rho_0 = \frac{2(2+m)\rho_{-2}}{2-m}, \quad (67)$$

then we can solve Eqs. (65) for $\rho_{\pm 2}$ and obtain ρ_0 from Eq. (67). For $2 > m > 0$ the spatial extent $(l_{\mathcal{D}(+2)})$ of density ρ_{+2} is larger than the spatial extent $(l_{\mathcal{D}(-2)})$ of density ρ_{-2}. Equations (65) can then be be solved to obtain

$$\rho_{+2}(X) = \frac{4c_1(m-2)(X^2-\delta) + c_0\kappa(6+m)}{64c_0c_1}, \quad X \leq l_{\mathcal{D}(-2)} \quad (68)$$

$$= \frac{2\mu_{+2} - X^2}{2\mathcal{C}_{II}}, \quad l_{\mathcal{D}(+2)} \geq X \geq l_{\mathcal{D}(-2)}, \quad (69)$$

$$\rho_{-2}(X) = \frac{(m-2)\big[c_0\kappa + 4c_1\{X^2-\delta\}\big]}{64c_0c_1}, \quad X \leq l_{\mathcal{D}(-2)}, \quad (70)$$

where $\delta = \mu_{+2} + \mu_{-2}, \kappa = \mu_{+2} - \mu_{-2}$. with the chemical potentials μ_{+2} and μ_{-2} given by

$$\mu_{+2} = \frac{l_{\mathcal{D}(+2)}^2}{2}, \quad \mu_{-2} = \frac{(c_0 - 4c_1)l_{\mathcal{D}(+2)}^2 + 8c_1 l_{\mathcal{D}(-2)}^2}{2\mathcal{C}_{II}}, \quad (71)$$

where $l_{\mathcal{D}(+2)}$ and $l_{\mathcal{D}(-2)}$ are the same as $l_{\mathcal{D}(+2)}$ and $l_{\mathcal{D}(-1)}$ of Eqs. (58)-(59), respectively. After substituting the expressions for chemical potentials $\mu_{\pm 2}$ given by Eqs. (71) in Eqs. (67)-(70), we obtain the final densities $\rho_{\pm 2}$ and ρ_0 as

$$\rho_{+2}(X) = \frac{c_0\left[8l_{\mathcal{D}(+2)}^2 - l_{\mathcal{D}(-2)}^2(6+m) + (-2+m)X^2\right]}{16c_0\mathcal{C}_{II}} + \frac{4c_1(2-m)(l_{\mathcal{D}(-2)}^2 - X^2)}{16c_0\mathcal{C}_{II}}, \quad X \leq l_{\mathcal{D}(-2)}, \quad (72)$$

$$\rho_{+2}(X) = \frac{l_{\mathcal{D}(+2)}^2 - X^2}{2\mathcal{C}_{II}}, \quad l_{\mathcal{D}(+2)} \geq X \geq l_{\mathcal{D}(-2)}, \quad (73)$$

$$\rho_0(X) = \frac{2(2+m)\rho_{-2}}{2-m}, \quad X \leq l_{\mathcal{D}(-2)}, \quad (74)$$

$$\rho_{-2}(X) = \frac{(2-m)\left(l_{\mathcal{D}(-2)}^2 - X^2\right)}{16c_0}, \quad X \leq l_{\mathcal{D}(-2)} \quad (75)$$

$$\rho_0(X) = \rho_{-2} = 0, \quad l_{\mathcal{D}(+2)} \geq X \geq l_{\mathcal{D}(-2)}. \quad (76)$$

The analytic and numerical densities in this case for a spin-2 quasi-1D ^{23}Na cyclic BEC are shown in Fig. 8.

The criteria for the validity of TFA in this case are again given by Eqs. (63)-(64) for $m_f = +2$ and $m_f = -2$ components, receptively. Thus, for a spin-2 ^{23}Na cyclic BEC, there are two distinct degenerate ground states as are shown in Figs. 7 and 8. The Hamiltonian of the spinor BEC is time-reversal invariant, yet the degenerate states shown in Figs. 7 and 8 break time reversal symmetry. Time-reversal symmetry-breaking states in spinor BECs were previously studied [15]. In cyclic phase too the additional potential energy cost rules out the possibility of asymmetric phase-separated profiles as ground states.

V. CONCLUDING REMARKS

The mean-field GP equation for a spin-1 and spin-2 spinor BEC involve three- and five-component complex wave function. Some simplification emerges for the ground-state wave function of a spinor BEC. For an anti-ferromagnetic or cyclic BEC with a non-zero magnetization, some of the spin-component wave functions become zero, thus reducing the original GP equation with three or five components to a system of coupled equations with only two or three components, which we call a reduced GP equation. For a ferromagnetic BEC with a non-zero magnetization the densities of different spin components for the ground-state wave function are found to be multiples of each other. This allows to solve the density according to a single GP equation, which we call the decoupled-mode (DM) equation, and calculate the densities of different spin components as multiples of a single DM density. These reduced GP and DM equations are valid in all spatial dimensions. Here we suggest simple analytic models for the ground-state densities of a spinor BEC obtained by applying Thomas-Fermi approximation to the DM and reduced GP equations. These analytic results for densities are found to be in good agreement with those obtained from the numerical solution of the full GP equation for ferromagnetic, anti-ferromagnetic, and cyclic spin-1 and spin-2 spinor BECs. Although, we considered in this paper nearly-overlapping configurations of the spinor components, the presence of Zeeman energy and spin-orbit coupling in the Hamiltonian can lead to asymmetric phase-separated configurations [13, 15] as ground states. An investigation leading to the analytic densities of the phase-separated solutions would be an interesting future work.

VI.   APPENDIX A

A.   Ferromagnetic spin-1 BEC

For the ground state of a spin-1 ferromagnetic BEC ($c_1 < 0$), the coefficients α_j, can be obtained from a minimization of the energy

$$E = \frac{N}{2} \int \Big[\sum_{j=-1}^{1} |\phi_j'|^2 + x^2\rho + c_0\rho^2 + c_1|\mathbf{F}|^2 \Big] dx, \quad (77)$$

where prime denotes x derivative. Assuming that component wave functions are given by the DM *ansatz* (12), to minimize energy E we need to maximize the positive integral $\int |\mathbf{F}|^2 dx$

$$\int |\mathbf{F}|^2 dx = [2|(\alpha_{+1}^*\alpha_0 + \alpha_0^*\alpha_{-1})|^2 + m^2]\mathcal{I}, \quad (78)$$

$$\mathcal{I} = \int \phi_{\mathrm{DM}}^4(x) dx. \quad (79)$$

Now, writing $\alpha_j = |\alpha_j|e^{i\theta_j}$, we get

$$\int |\mathbf{F}|^2 dx = \Big[2\big||\alpha_{+1}||\alpha_0| + |\alpha_0||\alpha_{-1}|e^{i(\theta_{+1}+\theta_{-1}-2\theta_0)}\big|^2 + m^2 \Big]\mathcal{I}. \quad (80)$$

To maximize integral (80), we take $\exp(\theta_{+1}+\theta_{-1}-2\theta_0) = 1$ and obtain

$$\int |\mathbf{F}|^2 dx = [2(|\alpha_{+1}||\alpha_0| + |\alpha_0||\alpha_{-1}|)^2 + m^2]\mathcal{I}. \quad (81)$$

For a fixed magnetization m and DM function ϕ_{DM}, the maximization of $\int |\mathbf{F}|^2 dx$ corresponds to finding the stationary points of the following "Lagrange" function

$$L_1(|\alpha_j|, \lambda_1, \lambda_2) = 2(|\alpha_{+1}||\alpha_0| + |\alpha_0||\alpha_{-1}|)^2 + \lambda_1(1 - \sum_j |\alpha_j|^2) + \lambda_2(m - |\alpha_{+1}|^2 + |\alpha_{-1}|^2). \quad (82)$$

Here λ_1 and λ_2 are Lagrangian multipliers to fix the normalization and magnetization to 1 and m, respectively. The stationary points of L_1 are determined by the following Lagrange equations

$$\frac{\partial L_1}{\partial |\alpha_j|} = 0, \quad \frac{\partial L_1}{\partial \lambda_1} = 0, \quad \frac{\partial L_1}{\partial \lambda_2} = 0. \quad (83)$$

with solution (14) together with $\lambda_1 = 2, \lambda_2 = -2m$.

B.   Anti-ferromagnetic spin-1 BEC

In case of an anti-ferromagnetic BEC ($c_1 > 0$), $\int |\mathbf{F}|^2 dx = \int (F_+F_- + F_z^2) dx$ is minimized by making $\phi_0(x) = 0$ for any $m \neq 0$ and the densities satisfy Eq.

(16). If we further assume the DM *ansatz* (12), the coefficients α_j can be obtained from a minimization of (80). For this, we take $\exp(\theta_{+1} + \theta_{-1} - 2\theta_0) = -1$ and obtain

$$\int |\mathbf{F}|^2 dx = [2(|\alpha_{+1}||\alpha_0| - |\alpha_0||\alpha_{-1}|)^2 + m^2]\mathcal{I}. \quad (84)$$

Following the procedure discussed for a ferromagnetic BEC, one can minimize $\int |\mathbf{F}|^2 dx$ under the twin constraints of fixed norm and magnetization and, in agreement with Eq. (16), obtain

$$|\alpha_{\pm 1}| = \sqrt{\frac{1 \pm m}{2}}, \quad \alpha_0 = 0. \quad (85)$$

VII.   APPENDIX B

A.   Ferromagnetic spin-2 BEC

For a spin-2 ferromagnetic BEC ($c_1 < 0, c_2 > 20c_1$), the energy is given by

$$E = \frac{N}{2} \int \Big[\sum_{j=-2}^{2} |\phi_j'|^2 + x^2\rho + c_0\rho^2 + c_1|\mathbf{F}|^2 + c_2|\mathbf{\Theta}|^2 \Big] dx.$$

For a ferromagnetic BEC, the energy minimization corresponds to a maximization of the c_1-dependent term $\int |\mathbf{F}|^2 dx$. We find that this automatically minimizes the c_2-dependent term $\int |\Theta|^2 dx$ to zero. Assuming the DM *ansatz* (23) we seek the coefficients α_j which maximize $\int |\mathbf{F}|^2 dx$. Following the procedure for ferromagnetic spin-1 BEC, we can write

$$\int |\mathbf{F}|^2 dx = \Big[\Big| 2\big\{ |\alpha_{+2}||\alpha_{+1}| + |\alpha_{-2}||\alpha_{-1}| e^{i(\theta_{-2}-\theta_{-1}-\theta_1+\theta_2)} \big\} + \sqrt{6} e^{i(\theta_0 - 2\theta_1 + \theta_2)} \big\{ |\alpha_{+1}||\alpha_0| + |\alpha_0||\alpha_{-1}| e^{i(\theta_{-1}-2\theta_0+\theta_1)} \big\} \Big|^2 + m^2 \Big]\mathcal{I}. \quad (86)$$

To maximize (86) we take all exponential factors in this equation to be $+1$ and obtain

$$\int |\mathbf{F}|^2 dx = \Big[\big\{ 2(|\alpha_{+2}||\alpha_{+1}| + |\alpha_{-2}||\alpha_{-1}|) + \sqrt{6}(|\alpha_{+1}||\alpha_0| + |\alpha_0||\alpha_{-1}|) \big\}^2 + m^2 \Big]\mathcal{I}. \quad (87)$$

For a fixed m ($2 > m > 0$) and $\mathcal{I}$, the maximization of $\int |\mathbf{F}|^2 dx$ corresponds to finding the stationary points of the following Lagrange function

$$L_2(|\alpha_j|, \lambda_1, \lambda_2) = 2(|\alpha_{+2}||\alpha_{+1}| + |\alpha_{-2}||\alpha_{-1}|) + \sqrt{6}|\alpha_0| (|\alpha_{+1}| + |\alpha_{-1}|) + \lambda_1(1 - \sum_j |\alpha_j|^2) + \lambda_2 (m - 2|\alpha_{+2}|^2 - |\alpha_{+1}|^2 + |\alpha_{-1}|^2 + 2|\alpha_{-2}|^2).$$

Here λ_1 and λ_2 have the same meaning as in Eq. (82). The stationary point which maximizes $\int |\mathbf{F}|^2 d\mathbf{x}$ thus yields Eqs. (24)-(26) together with

$$\lambda_1 = \frac{4}{\sqrt{(4-m^2)}}, \quad \lambda_2 = -\frac{m}{\sqrt{(4-m^2)}}. \quad (88)$$

Using Eqs. (24)-(26), we find that these α_j's also minimize $\int |\Theta|^2 d\mathbf{x}$ to 0 which guarantees that the state so obtained is the ground state.

B. Anti-ferromagnetic spin-2 BEC

Similarly in anti-ferromagnetic subdomain ($c_2 < 0$ and $c_2 < 20c_1$), the energy minimization corresponds to a maximization of the c_2-dependent term $\int |\Theta|^2 d\mathbf{x}$. Assuming DM *ansatz* (16) and $\alpha_j = |\alpha_j| \exp(i\theta_j)$ we have

$$\int |\Theta|^2 d\mathbf{x} = \big| 2|\alpha_{+2}||\alpha_{-2}| - 2|\alpha_{+1}||\alpha_{-1}| e^{i(\theta_1+\theta_{-1}-\theta_2-\theta_{-2})}$$
$$+ |\alpha_0|^2 e^{i(2\theta_0-\theta_2-\theta_{-2})} \big|^2 \mathcal{I}. \quad (89)$$

To maximize integral (89) we take the first exponential to be -1 and the second exponential to be $+1$. For a fixed m ($2 > m > 0$) and $\mathcal{I}$, the maximization of $\int |\Theta|^2 d\mathbf{x}$ corresponds to finding the stationary points of the following Lagrange function

$$L_\theta(|\alpha_j|, \lambda_1, \lambda_2) = (2|\alpha_{+2}||\alpha_{-2}| + 2|\alpha_{+1}||\alpha_{-1}| + |\alpha_0|^2)$$
$$+ \lambda_1(1 - \sum_j |\alpha_j|^2) + \lambda_2(m - 2|\alpha_{+2}|^2$$
$$- |\alpha_{+1}|^2 + |\alpha_{-1}|^2 + 2|\alpha_{-2}|^2). \quad (90)$$

The stationary point, which maximizes $\int |\Theta|^2 d\mathbf{x}$, yields

$$|\alpha_{\pm 2}| = \frac{\sqrt{2 \pm m}}{2}, \quad \alpha_{\pm 1} = \alpha_0 = 0, \quad (91)$$

$$\lambda_1 = \frac{2}{\sqrt{(4-m^2)}}, \quad \lambda_2 = \frac{-m}{2\sqrt{(4-m^2)}}. \quad (92)$$

Using Eqs. (91)-(92), we find that $\int |\mathbf{F}|^2 d\mathbf{x}$ has the minimum value $m^2 \mathcal{I}$ which guarantees that the state so obtained is the ground state.

C. Cyclic spin-2 BEC

For a spin-2 cyclic BEC $c_1 > 0$ and $c_2 > 0$, energy minimization involves minimization of both $\int |\mathbf{F}|^2 d\mathbf{x}$ and $\int |\Theta|^2 d\mathbf{x}$ to their respective minimum values $m^2 \mathcal{I}$ and 0, respectively. From equations (86) and (89), one can see that for $0 < m < 2$, consistent with Eqs. (31)-(32), there are only two possibilities for the ground states:

$$(i)|\alpha_{\pm 2}| = \frac{2 \pm m}{4}, \quad |\alpha_0| = \frac{\sqrt{4-m^2}}{\sqrt{8}}, \quad \alpha_{\pm 1} = 0,$$
provided that $\exp(2\theta_0 - \theta_{+2} - \theta_{-2}) = -1$, and

$$(i)|\alpha_{+2}| = \frac{\sqrt{1+m}}{\sqrt{3}}, \quad |\alpha_{-1}| = \frac{\sqrt{2-m}}{\sqrt{3}}, \quad \alpha_{\pm 1} = \alpha_0 = 0.$$

[1] D. M. Stamper-Kurn, M. R. Andrews, A. P. Chikkatur, S. Inouye, H.-J. Miesner, J. Stenger, and W. Ketterle, Phys. Rev. Lett. **80** 2027 (1998).
[2] Y. Kawaguchi and M. Ueda, Phys. Rep. **520**, 253 (2012).
[3] M. Ueda, Rep. Prog. Phys. **77**, 122401 (2014).
[4] D. M. Stamper-Kurn and M. Ueda, Rev. Mod. Phys. **85**, 1191 (2013).
[5] T. Ohmi and K. Machida, J. Phys. Soc. Japan **67**, 1822 (1998); T.-L. Ho, Phys. Rev. Lett. **81** 742 (1998).
[6] C. V. Ciobanu, S.-K. Yip, and T.-L. Ho, Phys. Rev. A **61** 033607 (2000);
[7] M. Ueda and M. Koashi, Phys. Rev. **A** 65 063602 (2002); H. Saito and M. Ueda, Phys. Rev. A **72** 053628 (2005).
[8] J. Stenger, S. Inouye, D.M. Stamper-Kurn, H.-J. Miesner, A.P. Chikkatur, and W. Ketterle, Nature **396**, 345 (1998).
[9] D. R. Romano and E. J. V. de Passos, Phys. Rev. A **70**, 043614 (2004); K. Murata, H. Saito, and M. Ueda, Phys. Rev. A **75** 013607 (2007).
[10] W. Zhang, S. Yi, and L. You, New J. Phys. **5**, 77 (2003).
[11] M. Matuszewski, T. J. Alexander, and Y. S. Kivshar, Phys. Rev. A 80, 023602 (2009); M. Matuszewski, Phys. Rev. A **82**, 053630 (2010).
[12] H. Wang, Int. J. of Computer Math. **84**, 925 (2007); W. Bao and F. Y. Lim, Siam J. Sci. Comp. **30**, 1925 (2008); F. Y. Lim and W. Bao, Phys. Rev. E **78**, 066704 (2008).
[13] S. Gautam and S. K. Adhikari, Phys. Rev. A **90**, 043619 (2014).
[14] H. Wang, J. Comput. Phys. **230**, 6155 (2011); **274**, 473 (2014).
[15] S. Gautam and S. K. Adhikari, Phys. Rev. A **91**, 013624 (2015).
[16] L. Salasnich, A. Parola, and L. Reatto, Phys. Rev. A **65**, 043614 (2002).
[17] G. Baym and C. J. Pethick, Phys. Rev. Lett. **76**, 6 (1996).
[18] F. Dalfovo, L. Pitaevskii, and S. Stringari, J. Res. Natl. Stand. Technol. **101,** 537 (1996); Rev. Mod. Phys. **71**, 463 (1999).
[19] C. J. Pethick and H. Smith, *Bose-Einstein condensation in dilute gases*, Cambridge University Press, Cambridge (2002).
[20] P. Schuck and X. Viñas, Phys. Rev. A **61**, 043603 (2000).
[21] T.-L. Ho and V. B. Shenoy, Phys. Rev. Lett. **77**, 3276 (1996); M. Trippenbach, K. Góral, K. Rzazewski, B. Malomed, and Y. B. Band, J. Phys. B **33**, 4017 (2000); S. T. Chui, V. N. Ryzhov, and E. E. Tareyeva, Phys. Rev. A

63, 023605 (2001); JETP Lett. **75**, 279 (2002); J. Polo, V. Ahufinger, P. Mason, S. Sridhar, T. P. Billam, and S. A. Gardiner, Phys. Rev. A **91**, 053626 (2015); S. Gautam and D. Angom, J. Phys. B **43**, 095302 (2010).

[22] J. Mur-Petit, Phys. Rev. A **79**, 063603 (2009).

[23] A. Aftalion and P. Mason, Phys. Rev. A **88**, 023610 (2013).

[24] E. G. M. Van kempen, S. J. J. M. F. Kokkelmans, D. J. Heinzen, and B. J. Verhaar, Phys. Rev. Lett. **88**, 093201 (2002);

[25] M.-S. Chang, Q. Qin, W. Zhang, L. You, and M. S. Chapman, Nature Phys. **1**, 111 (2005); A. Widera, F. Gerbier, S. Fölling, T. Gericke, O. Mandel, and I. Bloch, New J. Phys. **8**, 152 (2006).

[26] A. T. Black, E. Gomez, L. D. Turner, S. Jung, and P. D. Lett, Phys. Rev. Lett. **99**, 070403 (2007).

[27] S. Inouye, M. R. Andrews, J. Stenger, H.-J. Miesner, D. M. Stamper-Kurn, and W. Ketterle, Nature (London) **392**, 151 (1998).

[28] C. Chin, R. Grimm, P. Julienne, and E. Tiesinga, Rev. Mod. Phys. **82**, 1225 (2010).

[29] C. K. Law, H. Pu, and N. P. Bigelow, Phys. Rev. Lett. **81**, 5257 (1998); H. Pu, C. K. Law, S. Raghavan, J. H. Eberly, and N. P. Bigelow, Phys. Rev. A **60**, 1463 (1999).

[30] S. Yi, Ö. E. Müstecaplıoğlu, C. P. Sun, and L. You, Phys. Rev. A **66**, 011601(R) (2002).

[31] P. Muruganandam and S. K. Adhikari, Comput. Phys. Commun. **180**, 1888 (2009); D. Vudragovic, I. Vidanovic, A. Balaz, P. Muruganandam, and S. K. Adhikari, Comput. Phys. Commun. **183**, 2021 (2012).